Journal of The Electrochemical Society, **160** (11) H803-H812 (2013)
0013-4651/2013/160(11)/H803/10/$31.00 © The Electrochemical Society

Anodically Polarized Nickel Electrodes in DMSO or DMF Solutions of Pseudohalide Ions: IR Spectroelectrochemical Studies

L. K. H. K. Alwis,[a] Michael R. Mucalo,[a,z] and Bridget Ingham[b]

[a]*Chemistry Department, Faculty of Science and Engineering, The University of Waikato, Hamilton 3240, New Zealand*
[b]*Callaghan Innovation Research Limited, Lower Hutt 5040, New Zealand*

A novel subtractively normalized interfacial Fourier transform infrared spectroscopic (SNIFTIRS) investigation of anodically polarized nickel electrodes in pseudohalide-containing DMF or DMSO solutions (i.e. OCN^-, SCN^-, $SeCN^-$), in supporting electrolyte, tetrabutylammonium perchlorate (TBAP), is presented. In general, the data showed that nickel demonstrated irreversible anodic dissolution in all solutions studied at very high values of the applied potential, > +500 mV (AgCl/Ag). The predominant speciation of nickel in these systems was as complex ions consisting of Ni^{2+} ion complexed to pseudohalide ions and solvent molecules. Insoluble films and dissolved CO_2 were also detected, though mostly in the Ni/OCN^- systems studied. Ni(II)/pseudohalide complex ion species detected were modeled using solutions containing Ni^{2+} ion mixed with pseudohalide ion in different mole ratios. In general, the Ni/OCN^- electrochemical system behaved differently relative to those of Ni/SCN^- and Ni/$SeCN^-$ due to the difference in colors observed in cell solutions after SNIFTIRS experiments which was mirrored in the model solutions. Ni(II)-cyanate species had a different, coordination geometry and gave a characteristic bright blue color due possibly to $Ni(NCO)_4^{2-}$ ion while Ni(II) thiocyanate and selenocyanate complex ion species had octahedral coordination geometries containing solvent and one coordinated pseudohalide ion and formed greeny yellow solutions.
 [DOI: 10.1149/2.010311jes]

Manuscript submitted July 31, 2013; revised manuscript received September 3, 2013. Published September 11, 2013.

Much molecular information can be revealed in electrochemical systems due to the marriage of infrared (IR) spectroscopy with dynamic electrochemical techniques like voltammetry. IR spectroelectrochemical studies of a variety of systems have appeared in the last 2–3 decades.[1–14] In particular, subtractively normalized interfacial Fourier transform infrared spectroscopy (SNIFTIRS) has afforded valuable information on the species formed at an electrode/electrolyte interface when anodic dissolution of an electrode occurs. Previous work has also led to detection of electrosorbed species using special configurations.[14] However much useful information can still be obtained by monitoring solution species generated in the thin layer between the working electrode and the IR window using a simple thin layer electrochemical cell. Using this approach, we have studied several systems in past work[13,14] involving anodic dissolution of nickel in aqueous, cyanide and pseudohalide-containing electrolytes. Electrolytes containing -C≡N groups allow easy detection by IR spectroscopy because the ν(C≡N) stretch occurs in the 2500–1800 cm^{-1} area of the IR spectrum where few fundamental IR vibrations are detected.

Mucalo et al.[5] studied corrosion of Ni electrodes in aqueous KCN and detected $[Ni(CN)_4]^{2-}$ (2124 cm^{-1}), OCN^- (2168 cm^{-1}) and other species. Cyanide ion was observed to oxidize to OCN^- ion and then to CO_2 at anodic potentials. Interfacial pH changes in the thin layer during the SNIFTIRS experiment were indicated by detection of species such as HCN and HNCO (2256 cm^{-1}). Mucalo and Li[13] studied the anodic dissolution of nickel electrodes in aqueous pseudohalide-containing electrolytes and reported the formation of Ni(II) pseudohalide complex ions, i.e. Ni(II) complexes involving OCN^-, SCN^- and $SeCN^-$ ions which gave peaks at 2225 cm^{-1}, 2121 cm^{-1} and 2123 cm^{-1} respectively. Dissolved CO_2 (2343 cm^{-1}) was also detected and attributed to electro-oxidation of the cyanate ions at the electrode surface.

Spectroelectrochemical studies of pseudohalide electrolytes and their interaction with nickel electrodes are rare though, several in situ spectroelectrochemical Raman and IR studies have been reported.[15,16] Bron and Holze[17] reported spectra of surface-adsorbed species on the copper and gold electrodes and found that thiocyanate ions adsorbed over the whole polarizable potential range studied but that cyanate ions adsorbed mostly at anodic potentials. Kilmartin et al.,[15] using Raman spectroscopy studied CuSeCN film formation on a copper electrode from aqueous solutions and reported formation of porous films. A weak band due to Se-bound CuSeCN from the film was detected at 2164 cm^{-1}.

IR spectroelectrochemical or electrochemical only studies of nickel electrodes anodically polarized in pseudohalide ion-containing *non-aqueous* solvent media such as dimethyl formamide (DMF) or dimethyl sulfoxide (DMSO), have not been previously reported in the literature. Instead, studies of Ni electrodes in mixed electrolytes of DMSO, DMF and aqueous acids exist. Delgado et al.[18] report that nickel electrodes in DMSO/HCl electrolytes exhibit distinct dissolution and passivation regions with passivation films consisting of an insoluble Ni(II) salt such as when ClO_4^- ion is present forming $Ni(DMSO)_6(ClO4)_2$. They comment that this is preceded by an irreversible active dissolution process where Ni(II)-DMSO complex ions form. Bellucci et al.[19] studied the passivation of nickel electrodes in 0.1 mol L^{-1} aqueous H_2SO_4 and acetonitrile and DMF solutions and found that water content strongly affected the passivation process because the NiO/ $NiSO_4$ film was of poor protective character. Abrashkina et al.[20] studied the anodic behavior of Ni electrodes in acidic perchlorate solutions of DMSO showing that anodic dissolution rate for Ni was much lower in DMSO than in water or DMF solvents. This was due to the strong adsorption of DMSO to the nickel surface. It was also shown that addition of surface activators like Cl^- and water molecules can substantially increase the rate of dissolution of nickel to the point of electrode pitting. Passivation by strong adsorption of DMSO to Ni was envisioned to occur via interaction of Ni with the oxygen atom on DMSO causing substantial loss of the double bond character of the S=O group. In contrast, for DMF or acetonitrile (AN), interaction with Ni occurs via the N-atom and no passivation occurs. Ercolano et al.[21] state that properties of organic solvents like dielectric constant, dipole moment and values of acid dissociation constants (if ionisable species are present like SO_4^{2-}) strongly influence electrochemical and corrosion behavior of metals in non-aqueous organic solvents. Banas et al.[22] investigated the corrosion and passivity of nickel in pure (non-aqueous) methanol solutions of electrolytes due to the application of alcohols to chemical engineering-related areas such as oxide nanoparticle synthesis, use as fuels and others. In methanol, Ni passivates via direct interaction with the oxygen in the methanol solvent to form a nickel(I) methoxide species which then loses a further electron to form a Ni(II) methoxide species.

IR spectroelectrochemical studies on nickel/pseudohalide systems and their speciation in DMF or DMSO solvents are of interest for understanding the electrochemistry of non-aqueous electrolyte systems used in different technical areas such as in the chemical and fiber industries.[21,23] Previous literature existing on

[z]E-mail: m.mucalo@waikato.ac.nz

the inorganic solution chemistry, spectroscopy and thermodynamics of the interaction of nickel ions and other transition metals with pseudohalide ions in DMF and DMSO solvents[24,25] assists such studies.

The aim of this paper is, therefore, to study using SNIFTIRS the anodic polarization of nickel electrodes in DMSO or DMF solutions of pseudohalide (OCN^-, SCN^-, $SeCN^-$) ions using tetrabutylammonium perchlorate as the supporting electrolyte. Conventional transmission IR and U.V./Vis. Spectrophotometry are also used for study of model solutions that serve to confirm the identity of species detected as a result of electrochemical processes.

Materials and Methods

Reagents and solutions.— DMF (Ajax Finechem Pty, analytical (UNIVAR) reagent grade) and DMSO (Scharlau, synthesis grade) solvents were used without further purification for all experimental work. The level of water impurity in the DMSO and DMF was quoted as being 0.1% and 0.15% respectively by Karl Fischer Titration. All glassware used was cleaned thoroughly, prior to commencing experiments. Sodium hydroxide (NaOH, >99.5% (Merck), potassium selenocyanate (KSeCN, >97.0%), tetrabutylammonium perchlorate (TBAP, >97.0%) were supplied by Aldrich Chemical Co, USA. Other salts, i.e. ($Ni(NO_3)_2.2H_2O$, >99%), sodium thiocyanate (NaSCN, >98%) and potassium cyanate (KOCN, >98.0%) were all sourced from BDH chemicals. Apart from the hydrated nickel(II) salts, all were used as-received from the manufacturer without further purification.

Prior to their use in preparation of model solutions, the hydrated nickel(II) nitrate salt was dehydrated in an oven (50°C) for 3–5 hours. In general, electrolyte solutions prepared for SNIFTIRS experiments had a concentration of either 0.025 or 0.05 mol L^{-1} in the pseudohalide salt and 0.1 mol L^{-1} in TBAP, the supporting electrolyte in the DMF or DMSO solvent.

Spectroelectrochemical cell and electrode cell design.— The working electrode was a flat, circular polycrystalline piece of (BDH)nickel (7 mm diameter) embedded into a glass syringe barrel using Araldite epoxy glue. The preparation of this electrode and its polishing are as described earlier.[13]

The thin layer IR spectroelectrochemical cell used in this study (see Fig. 1) was modeled on the specialized three electrode thin layer cell used in an earlier study.[13] The difference in design in the present study involved optimisation of the Luggin capillary which allowed more favorable placement of the reference electrode relative to the working electrode (see Fig. 1) and better maintenance of the electrolyte level in the Luggin capillary due to natural equilibration. The thin layer cell was placed on a fixed angle (30°) Spectra Tech FT-30 specular reflectance accessory as used in previous studies.[13]

Instrumentation.— All cyclic voltammetry was carried out using an EDAQ computer controlled potentiostat system controlled by Echem software as described previously.[13] The reference electrode used was AgCl/Ag and the counter electrode a platinum ring electrode. In studying a typical electrochemical system, a preliminary cyclic voltammetric characterization was carried out via a one sweep cycle from −800 mV to 2000 mV (AgCl/Ag). All SNIFTIRS spectra were obtained using a dry-N_2-purged Biorad FTS-40 FTIR spectrometer as described earlier[13] using either a liquid N_2-cooled MCT (mercury cadmium telluride) or InSb (indium antimonide) detector.

The details of the spectral acquisition technique for SNIFTIRS have been described in a previous study,[13] the potential used for acquiring background spectra was −900 mV (AgCl/Ag). SNIFTIRS spectra were then acquired at more anodic potentials. All in situ spectra were acquired at 4 cm^{-1} resolution for 100 scans. Additional to the preliminary CV characterization of the systems, current-potential data were collected at the same time as the SNIFTIRS by summing the initial current observed at the beginning of an IR spectral acquisition (at a given potential value) and at the end of that same acquisition and computing an average that was later plotted vs. the applied potential. These effectively represented "slow" "single sweep" voltammograms (i.e. like linear sweep voltammograms) of the nickel / pseudohalide systems but recorded over the timescale of the SNIFTIRS experiment.

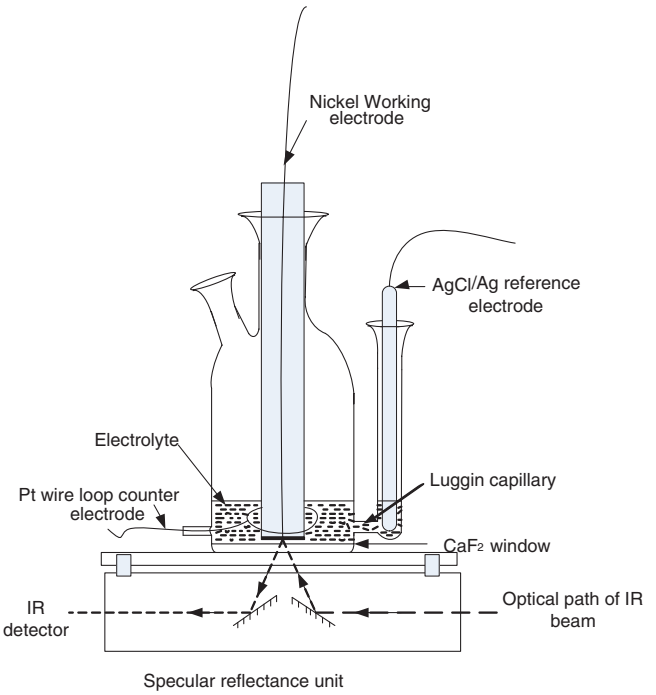

Figure 1. Schematic of the three electrode thin-layer IR spectroelectrochemical used.

The thickness of the thin layer was determined by obtaining the Beer's law plot of five accurately known concentrations of potassium ferricyanide (BDH Anala-R grade)) between 0.025 mol L^{-1} and 0.4 mol L^{-1} in water via IR absorbance measurements of the $\nu(C{\equiv}N)$ stretching peak of the $Fe(CN)_6^{3-}$ ion peak at 2114 cm^{-1} from solutions held in a Buck Scientific fixed pathlength cell using two 32 × 3 mm CaF_2 windows and a Teflon 0.015 mm spacer. The extinction coefficient measured from this graph and accounting for solution thickness (0.0015 cm) was used to determine the thickness of the thin layer cell employed in experiments by measuring the intensity of the same five accurately known concentrations of potassium ferricyanide in the thin layer cell set up on the specular reflectance unit and calculating it from the slope of the Beer's Law plot obtained. As a double pass of the IR beam is involved in the thin layer cell (i.e. the IR beam enters the thin layer cell and then emerges again by reflection off the working electrode surface), the measured absorbances were divided by two before plotting them on the Beer's Law graph of absorbance vs. concentration. This led to a value of 1.31 μm which is a realistic estimate of a thin layer cell thickness.[2]

In addition, experiments were done to confirm the CVs were similar when a thin layer and a thicker layer of electrolyte was maintained between the electrode and the IR window during potential sweeps. The thicker layer was created by lifting the Ni working electrode to a distance of 1 cm above the IR window and fixing it in place before acquisition of the CV. This was done to confirm bulk solution properties in the thin layer.

IR spectra of *model solutions* consisting of mixtures of Ni(II) salt and pseudohalide ions at various Ni(II):pseudohalide ion mole ratios were recorded in conventional IR transmission mode between CaF_2 windows as described previously[13] but were acquired on a Perkin Elmer Spotlight 200 FTIR instrument with a Spectrum 400 optical bench and a conventional DTGS room temperature detector.

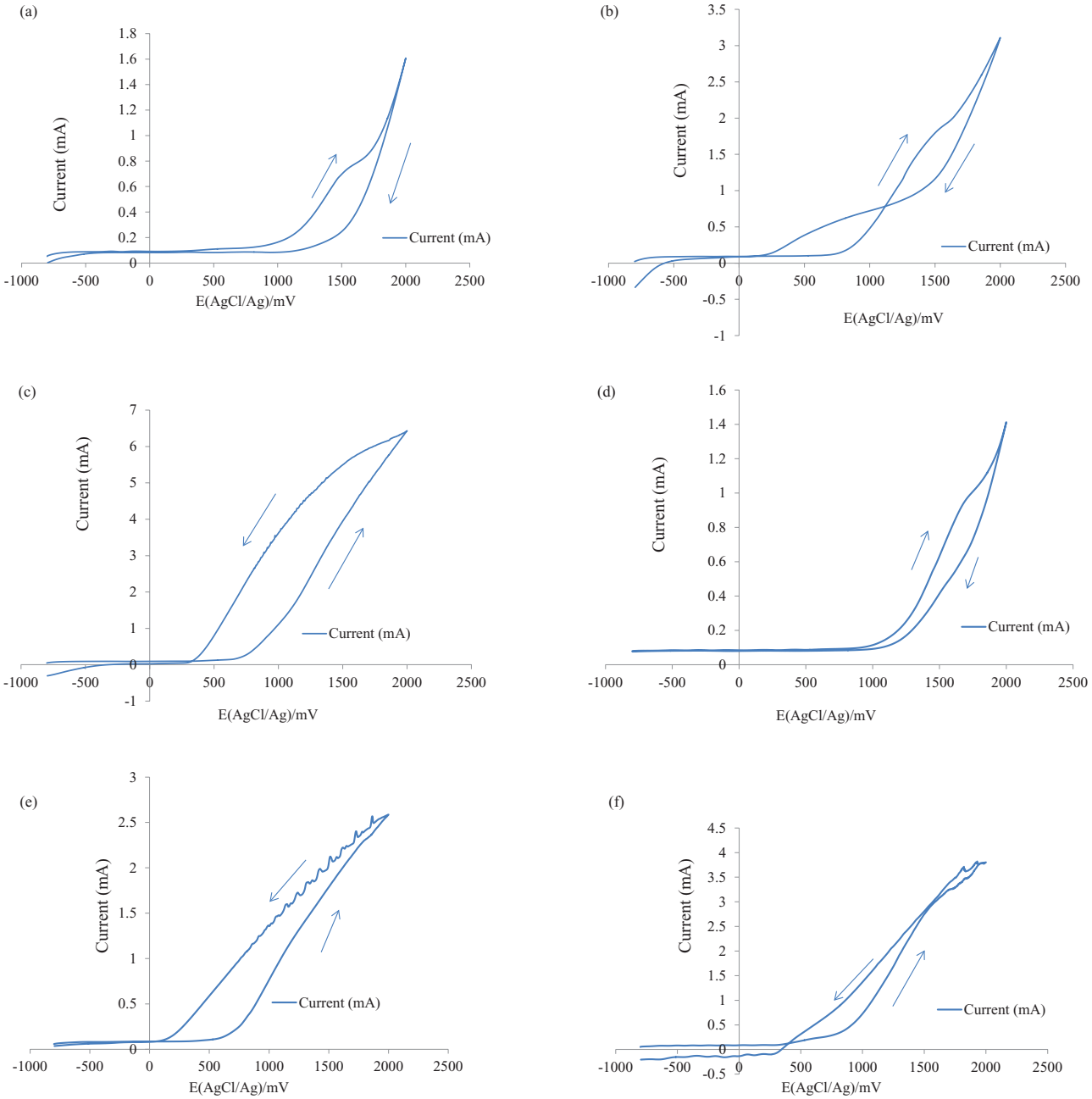

Figure 2. Cyclic voltammograms of the nickel electrode in DMF and DMSO solvents containing pseudohalide ions and 0.1 mol L^{-1} TBAP (sweep rate = 20 mV/s): (a) 0.025 mol L^{-1} KOCN in DMF, (b) 0.05 mol L^{-1} NaSCN in DMF, (c) 0.05 mol L^{-1} KSeCN in DMF, (d) 0.025 mol L^{-1} KOCN in DMSO, (e) 0.05 mol L^{-1} KSCN in DMSO and (f) 0.05 mol L^{-1} KSeCN in DMSO. Arrows show the path actually traced upon conducting the sweep of potentials.

All U.V./Vis. spectra of model solutions and solutions from the electrochemical cell after SNIFTIRS experiments were acquired for qualitative assessments of species without baseline correction using a double beam Cary 1E UV-VIS spectrophotometer with a combined Tungsten and Hydrogen-Deuterium source. Scanning conditions used a data interval of 1 nm and a scanning rate of 600 nm/min. All samples were placed in 1 cm pathlength quartz cuvettes and spectra acquired over the 800–200 nm range. The reference (blank) solvent used was DMF or DMSO depending on the samples being analyzed.

Results and Discussion

Cyclic voltammetry of the Ni electrode systems in DMF and DMSO in the presence of cyanate, thiocyanate and selenocyanate.— The CVs for the Ni electrode systems anodically polarized in DMF and DMSO solutions of pseudohalide ions (OCN^- (0.025 mol L^{-1}), SCN^-, and $SeCN^-$ (both 0.05 mol L^{-1})) containing 0.1 mol L^{-1} tetrabutylammonium perchlorate as an inert supporting electrolyte are shown in Fig. 2a-2f. The voltage was adjusted between −800 mV(AgCl/Ag) and +2000 mV(AgCl/Ag). CVs of all systems studied exhibited a featureless low current "flat" region from −800 mV(AgCl/Ag) to +500 mV(AgCl/Ag). Studies on related electrochemical systems studied in DMSO[20] solvents suggest that solvent adsorption of DMSO inhibits surface reactions on the nickel electrode in this potential region which may explain the existence of featureless regions in the CV. The same may be said of the systems in the DMF-based solvents.

After *ca.* +500 mV(AgCl/Ag) (Fig. 2), the nickel electrode entered its "active dissolution region" where current was observed to rise significantly and continuously until the voltage was reversed at +2000 mV(AgCl/Ag) and returned to the starting voltage. In this

region, Ni is being oxidized to Ni(II) and other processes such as solvent oxidation, pseudohalide ion oxidation and film formation are occurring at the electrode surface. For instance, cyanate ion would be subject to oxidation to CO_2.

Hysteresis was apparent in CVs of all systems studied (see arrows indicating forward and backward sweeps in Figs. 2b, 2c, 2e and 2f) except in systems involving OCN^- ion (Fig. 2a and Fig. 2d) where the reason for this was not immediately clear given the nickel electrode was also actively dissolving in this system. This may be related to the electrode kinetics of the system under the scanning conditions of the CV. Hysteresis clearly indicated that the surface of the electrode was not being restored to what it was before anodic polarization and that reactions occurring in the anodic dissolution process after +500 mV(AgCl/Ag) were irreversible. CVs recorded of the Ni/SCN^-/DMSO and Ni/$SeCN^-$/DMSO systems (Fig. 2e and 2f) also showed (on the return sweep of the CV) some random fluctuations in current. These were confirmed to be random when repeated and compared and furthermore also occurred when the system was connected to a different potentiostat. The cause is unknown but speculated to be flaking or loss of a layer or film (as it is reduced on the reverse voltage sweep back to metal or other species) of insoluble nickel salt generated on the forward voltage sweep though visible evidence of this film was lacking.

In the region of the CV where active dissolution occurs (see Fig. 2) and given the voltage sweep was taken to a maximum of +2.0 V, part of the current increase must also be attributed to solvent oxidation on the Ni electrode in all systems studied. Krtil et al.[26] report that DMSO oxidizes to dimethyl sulfone on Pt and other electrodes supported by $LiClO_4$-containing electrolytes at +1.3 V with respect to a saturated calomel electrode (SCE) reference which corresponds to +1.36 V (AgCl/Ag) so lending support to solvent oxidation occurring in the present systems. Likewise, sharp increases in current after +1500 mV(AgCl/Ag) in the Ni/DMF/pseudohalide ion systems can also be partially attributable to the oxidation of DMF solvent.

IR spectra of all systems.— The SNIFTIRS spectra of all systems investigated are presented in Fig. 4a to 4f. Single sided voltammograms which represent the average potential/current data collected during each SNIFTIRS experiment are shown in Fig. 3a to 3f while intensity-potential plots showing how detected species from SNIFTIRS spectra in each system varied with applied potential are displayed in Fig. 5a to 5f. Table I summarizes the IR (and UV/Vis) data from the 6 SNIFTIRS experiments done in DMSO and DMF solvents with each of the pseudohalide ions in contact with the nickel electrode. Data for the systems are presented together due to the commonality of trends in spectroscopic behavior observed between the different systems investigated.

In general, all systems studied gave relatively featureless IR spectra in the cathodic polarization region (i.e. up to 0 mV(AgCl/Ag). Positive going peaks due to free pseudohalide ion in the thin layer were rarely detected because it was more common to observe a *negative* going peak (see Fig. 4a to 4f). Negative going peaks are observed because the intensity of the free pseudohalide ion at the background potential of −900 mV(AgCl/Ag) exceeds what it is at more anodic potentials where it is being consumed (see later). Supporting this, intensity-potential plots (Fig. 5a to 5f show clearly that the peak intensity due to free pseudohalide ion in all systems studied becomes increasingly negative in the anodic polarization region up until very high anodic voltages where it levels off and fluctuates due most likely to disturbances in the thin layer caused by gas evolution. Most features of interest in the SNIFTIRS spectra occurred in the anodic polarization region after 0 mV (AgCl/Ag). This is reflected by the single sided voltammograms of the systems studied (Fig. 3a to 3f which all demonstrate significant current increases. The major feature observed in all SNIFTIRS spectra of systems studied was a peak due to a Ni(II) complex ion incorporating coordinated solvent and pseudohalide ion from the solvent which depending on the system was detected between 2094 and 2200 cm^{-1} (see Table I, Fig. 3). These are due to the nickel electrode producing Ni^{2+} ions which subsequently complex with pseudohalide ion and solvent molecules from the electrolyte. In general, Ni(II) complexes involving OCN^- ion (see Fig. 4a and Fig. 4d) were invariably ∼100 cm^{-1} higher in vibrational frequency than the corresponding Ni(II) complexes containing SCN^- or $SeCN^-$ ions which typically occurred at ∼2100 cm^{-1}. At this stage, the exact stoichiometry of the Ni(II) complex with the pseudohalide ions, SCN^- or $SeCN^-$ and solvent (DMSO or DMF) (which may vary due to influence of complex equilibria) was speculated to be $[Ni(\text{pseudohalide ion})_x(\text{solvent})_{6-x}]^{(2-x)+}$. However the stoichiometry of the Ni(II) cyanate ion was found to be different. In situ investigations into the stoichiometries of the electrogenerated ions in solution are ongoing and will be covered in a separate publication.[27]

When the Ni(II)/pseudohalide complex ion forms in each of the systems studied by SNIFTIRS, the anodic polarization produces a very distinct color change in the electrochemical cell solution at the conclusion of the experiment. In general, all Ni/OCN^- systems studied produce a characteristic clear blue color whilst those of Ni/SCN^- or Ni/$SeCN^-$ produce a more insipid yellow-green color.

In SNIFTIRS spectra, as stated earlier, the peak due to the Ni(II)/pseudohalide complex ion was invariably detected when the Ni electrode was anodically polarized with a first appearance being noted in the range +200–+500 mV(AgCl/Ag). Given the E^0 value of the Ni^{2+}/Ni couple is known to be −0.25 V (NHE),[28] this shows that a large degree of polarization must occur for these Ni electrodes in non-aqueous DMF and DMSO electrolyte media before IR detectable species are observed. Previous workers have noted the large degree of cathodic polarization when reporting on the electrochemical *deposition* of Ni in mixed solvent media which contain DMSO or DMF[29] which was attributed to the stability of the $[Ni(DMSO)_6]^{2+}$ and $[Ni(DMF)_6]^{2+}$ ions and other species which tended to adsorb to the electrode surface. The intensity trends of the Ni(II)/pseudohalide complex ion-associated peaks observed in SNIFTIRS spectra shown in Fig. 4a to 4f can be viewed in Fig. 5a to 5f. For Ni/DMSO *or* DMF/OCN^- systems, the intensity of the Ni(II)/cyanate ion associated peak (∼2200 cm^{-1}) reached a maximum at ca. +1250 mV(AgCl/Ag) whilst the maximum intensity of the Ni(II)/thiocyanate complex ion in DMSO and DMF (∼2094 cm^{-1}) peak, occurred at ca. +1500 mV (AgCl/Ag) although in the Ni/SCN^-/DMSO system (Fig. 5e) there were fluctuations in intensity caused most likely by disturbances in the thin layer such as gas evolution that would have altered the thin layer composition. For the Ni/$SeCN^-$/DMF system (Fig. 5c) studied similar fluctuations in the intensity-potential plots were observed with a plateau in the intensity of the peak due to the Ni(II)/SeCN complex ion plateauing at +1750 mV(AgCl/Ag). In the Ni/$SeCN^-$/DMSO system (Fig. 5f), the intensity of the peak due to the Ni(II)/$SeCN^-$ complex ion did not plateau or show a maximum but was monotonically increasing even at +2000 mV(AgCl/Ag) when the SNIFTIRS experiment was terminated.

The intensity behavior observed for the Ni(II)/pseudohalide ions in all the systems studied, i.e increasing to a maximum and then declining (see Fig. 5a to 5e), has been tentatively attributed to the formation of an insoluble film on the electrode which forms at very high applied potentials. Spectroscopic evidence for this in the SNIFTIRS spectra of the Ni/OCN^- systems is provided by the appearance of a weak peak at 2244–2250 cm^{-1} at +1000–1300 mV(AgCl/Ag). Further voltammetric evidence is seen in the single sided voltammograms of the Ni/OCN^- systems (see Fig. 3a and 3d) in both DMF and DMSO where the current is observed to peak (very clearly in the Ni/OCN^-/DMF system) or form a shoulder (as in the Ni/OCN^-/DMSO system) which is attributable to solid film formation on the electrode.[5] In addition, Ni electrodes inspected after a SNIFTIRS experiment in Ni/OCN^-/DMF or Ni/OCN^-/DMSO systems show visible evidence of a film. The IR peak at 2244–2250 cm^{-1} suggests the surface film may contain nickel oxide and cyanate ion though its nature is unknown. Previous workers[30] studying α-$Ni(OH)_2$ and Ni-Al layer double hydroxides (LDHs) precipitated by urea have assigned peaks of this value to intercalated cyanate ion in nickel hydroxide film in which cyanate ion is O-bonded to Ni rather than N-bonded.

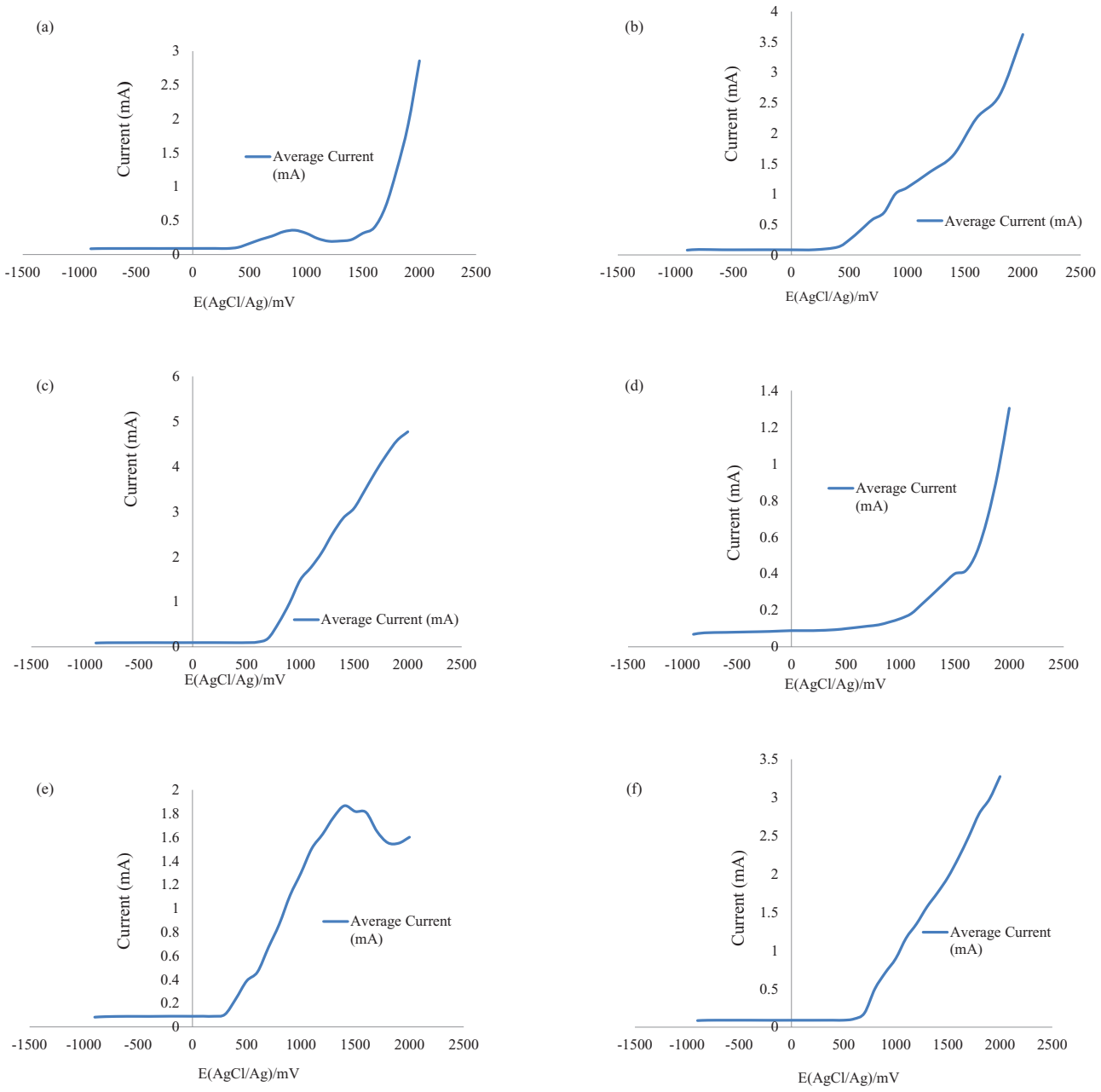

Figure 3. Single sweep voltammograms acquired of the nickel electrode over the timescale of a SNIFTIRS experiment in DMF and DMSO solvents containing pseudohalide ions and 0.1 mol L^{-1} TBAP: Data were obtained from calculating the average current at the beginning and end of the spectral acquisition period for each applied potential at which SNIFTIRS spectra were acquired. (a) 0.025 mol L^{-1} KOCN in DMF, (b) 0.05 mol L^{-1} NaSCN in DMF, (c) 0.05 mol L^{-1} KSeCN in DMF, (d) 0.025 mol L^{-1} KOCN in DMSO, (e) 0.05 mol L^{-1} NaSCN in DMSO and (f) 0.05 mol L^{-1} KSeCN in DMSO.

Aside from peaks attributable to Ni(II) complex ion species, another peak of low intensity which appeared at very high anodic applied potentials was commonly observed at 2337–2339 cm^{-1} (see Fig. 4a to 4f). This was assigned to CO_2 dissolved in the DMSO or DMF solvent, as the identically assigned species had been detected at 2343 cm^{-1} in the previously reported Mucalo and Li[13] SNIFTIRS study of Ni/pseudohalide ion systems in aqueous electrolytes. In the Ni/OCN^-/DMSO system, the peak due to CO_2 first appeared at +1000 mV (AgCl/Ag) and was present until +2000 mV(AgCl/Ag). The intensity of the CO_2-associated peak (see Fig. 5a and 5d) paralleled the rise in intensity of the peak at 2244 cm^{-1} which has been attributed earlier to an insoluble cyanate-containing nickel oxide film on the electrode. Similar observations with respect to the intensity of the CO_2-associated peak in the Ni/OCN^-/DMF system were also made. The 2337–2339 cm^{-1} peak was also observed in the SNIFTIRS spectra of the Ni/SCN^-/(DMSO or DMF) and $Ni/SeCN^-$/(DMSO or DMF) systems. Compared to the Ni/OCN^- systems, the intensity of the 2337–2339 cm^{-1} peak due to CO_2 was relatively lower and may have arisen solely through oxidation of the supporting solvent itself at the electrode surface at very anodic potentials. Krtil et al.[31] reported that acetonitrile oxidation to CO_2 on Pt, glassy carbon and anatase electrodes was initiated by trace water breakdown in the solvent. In the present study, DMF solvent oxidation may be inferred as a source of CO_2 but not in DMSO, where the principal breakdown product on Pt, glassy carbon and anatase electrodes is dimethyl sulfone.[26]

Table I. FTIR and U.V./Vis. data from in situ IR spectroelectrochemical studies of Ni/pseudohalide ion systems electrochemically polarized in 0.1 mol L^{-1} TBAP in DMSO or DMF solvents.

System studied	ν(CN) of free pseudohalide ion cm^{-1}	ν(CN) of Ni^{2+}-pseudohalide/solvent complex ion species or solid film[1] species cm^{-1}	ν(CO) of CO_2 dissolved in solvent cm^{-1}	U.V./Vis. spectral features (nm)	Color of cell solution after SNIFTIRS experiment
Ni/OCN^-/DMF	2134	2200, 2250[1]	2337	280 s, 430 w, 648 m, 670 m	blue
Ni/SCN^-/DMF	2056	2092	2339	271 s, 403 w,	light green
Ni/$SeCN^-$/DMF	2064	2094	2337	278 s, 397 w	yellow green
Ni/OCN^-/DMSO	2136	2199, 2244[1]	2337	273 s, 430 w, 602 m, 650 m	blue
Ni/SCN^-/DMSO	2055	2094	2337	265 s, 404 w	light green
Ni/$SeCN^-$/DMSO	2065	2095	2337	275 s, 401 w	yellow green

s = strong, m = medium, w = weak
[1] Refers to the CN stretching frequency of the solid film on the electrode

Transmission IR and U.V./Vis. Spectra of model solutions and cell solutions after the SNIFTIRS experiments.— Model solutions formed by mixing solutions of Ni(II) nitrate with solution of the pseudohalide salts were investigated by transmission IR spectroscopy and U.V./Vis spectrophotometry to provide confirmation of assignments of peaks to electrogenerated species of Ni(II) salts observed in the SNIFTIRS studies. The results of this work are summarized in Table II.

When making the solutions, the mole ratios of Ni(II) salt to pseudohalide ion were varied from 1:1 to 1:2 in DMF (due to solubility issues of salts concerned in DMF) while in DMSO solutions with Ni(II) salt: pseudohalide ion mole ratios varying from 1:1 to 1:8 were able to be prepared due to the better solubility of the salts in this solvent. The variation of the Ni(II) salt: pseudohalide salt mole ratio was carried out in order to investigate changes in these model solutions with respect to: 1) spectroscopic peaks observed in transmission IR and UV/Vis spectra and 2) the color of the resultant model solutions and their relationship to the observed SNIFTIRS spectra and resultant cell solution colors of the systems after the SNIFTIRS experiments.

Fig. 6 illustrates the transmission IR spectra of the 1:2 mole ratio Ni(II) : OCN^-, 1:1 mole ratio Ni(II): SCN^- and Ni(II):$SeCN^-$ model solutions in DMF. Fig. 7 illustrates the UV/Vis spectra of some selected model solutions from this study.

Ni(II)/OCN^- model solutions in DMSO and DMF: FTIR and UV/Vis data.— IR data for these systems in DMF indicate that a broad peak is observed at 2210 cm^{-1} for the 1:1 mole ratio solution (blue green color) which shifts to 2200 cm^{-1} in the 1:2 mole ratio solution (dark blue color). In DMSO, the observations were practically identical with the 1:1 (yellow green) and 1:2 mole ratio (blue-green) model solutions giving a peak at 2210 cm^{-1} which shifted to 2199 cm^{-1} in the 1:2 mole ratio solutions. This peak can be clearly assigned to the CN stretching frequency of a Ni/OCN^- complex that has formed in solution. In DMSO, the solubility of KOCN was higher and so two further model solutions were able to be prepared at 1:4 and 1:8 mole ratios. Both of these solutions were characteristically dark blue in color and both IR spectra indicated a peak unchanged in value from

Table II. FTIR and U.V./Vis. data from IR studies of DMF or DMSO model solutions of $Ni(NO_3)_2$ and potassium (or sodium) pseudohalide ion salts prepared with different mole ratios.

Model solution studied and mole ratio of ($Ni(NO_3)_2$): pseudohalide ion prepared in DMF or DMSO	ν(CN) of free pseudohalide ion cm^{-1}	ν(CN) of Ni^{2+}-pseudohalide complex ion species cm^{-1}	U.V./Vis spectral features nm	Observed color of solution
DMF				
$Ni(NO_3)_2$/ KOCN 1:1	nd	2210	276 s, 412 m, 602 w, 656 w	blue-green
$Ni(NO_3)_2$/ KOCN 1:2	nd	2200	280 s, 416 w, 600 s, 647 s	dark blue
$Ni(NO_3)_2$/ NaSCN 1:1	2056	2094	280 s, 404 m, 677 w	light green
$Ni(NO_3)_2$/ NaSCN 1:2	2056	2094	280 s, 404 m, 681 w	green
$Ni(NO_3)_2$/ KSeCN 1:1	2065	2098	288 s, 401 m, 680 w	yellow green
$Ni(NO_3)_2$/ KSeCN 1:2	2065	2098	292 s, 401 m, 675 w	light green
DMSO				
$Ni(NO_3)_2$/ KOCN 1:1	nd	2210	262 s, 418 m,	yellow-green
$Ni(NO_3)_2$/ KOCN 1:2	nd	2199	280 s, 426 w, 602 s, 649 s	blue-green
$Ni(NO_3)_2$/ KOCN 1:4	2137	2199	281 s, nd, 601 s, 648 s	dark blue
$Ni(NO_3)_2$/ KOCN 1:8	2137	2199	281 s, nd, 601 s, 649 s	dark blue
$Ni(NO_3)_2$/ NaSCN 1:1	2055	2094	263 s, 416 m, 700 w	light green
$Ni(NO_3)_2$/ NaSCN 1:2	2055	2094	266 s, 415 m, 701 w	green
$Ni(NO_3)_2$/ NaSCN 1:4	2055	2094	271 s, 415 m, 701 w	green
$Ni(NO_3)_2$/ NaSCN 1:8	2055	2094	273 s, 415 m, 700 w	green
$Ni(NO_3)_2$/ KSeCN 1:1	2065	2096	272 s, 412 m, 695 w	yellow green
$Ni(NO_3)_2$/ KSeCN 1:2	2065	2096	273 s, 416 m, 697 w	light green
$Ni(NO_3)_2$/ KSeCN 1:4	2065	2096	277 s, 416 m, 705 w	light green
$Ni(NO_3)_2$/ KSeCN 1:8	2065	2096	297 s, 416 m, 705	light green

s = strong, m = medium, w = weak

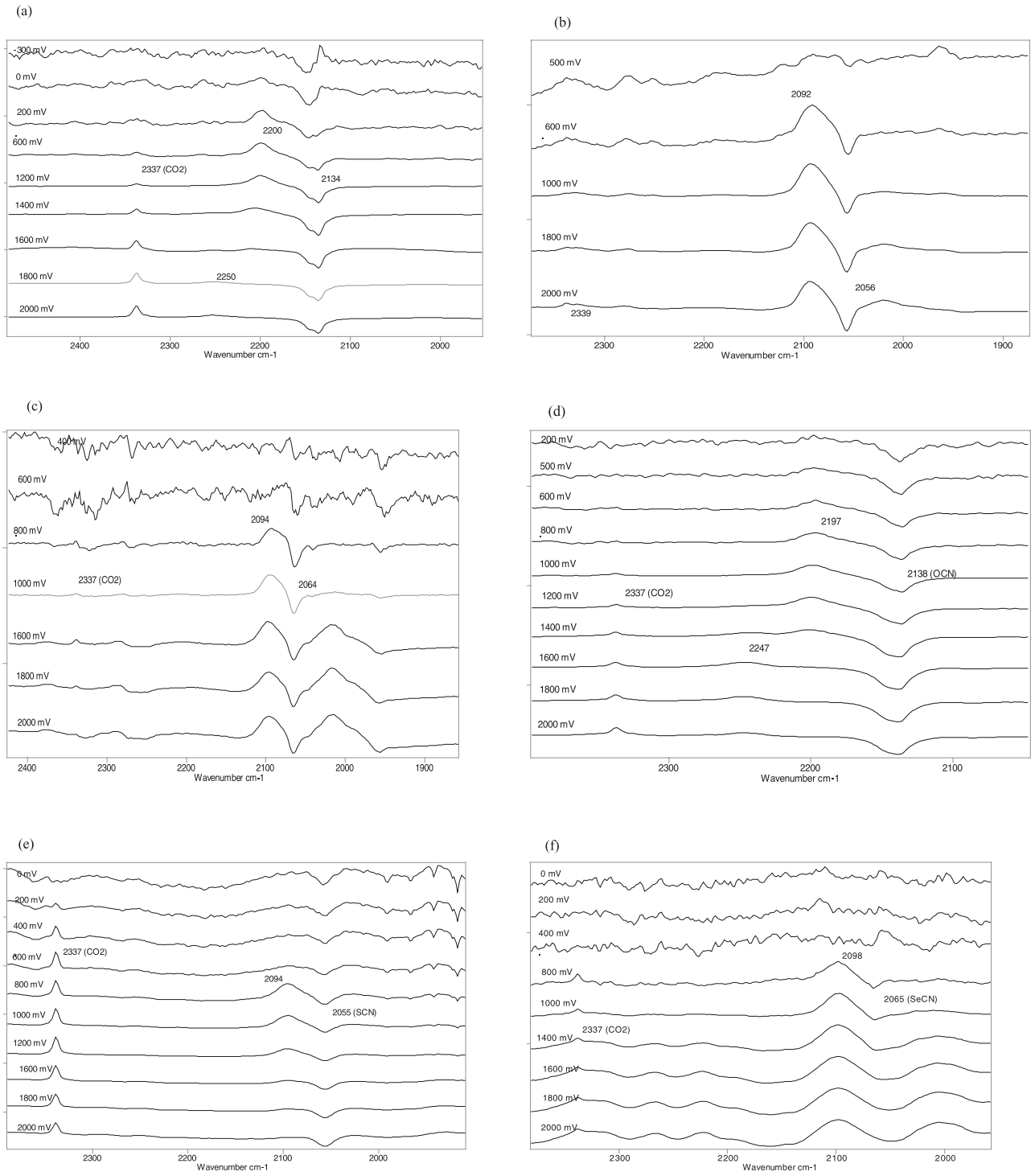

Figure 4. Series of SNIFTIRS spectra of the nickel electrode as a function of applied potential in DMF and DMSO solvents containing pseudohalide ions and 0.1 mol L^{-1} TBAP. (a) 0.025 mol L^{-1} KOCN in DMF, (b) 0.05 mol L^{-1} NaSCN in DMF, (c) 0.05 mol L^{-1} KSeCN in DMF, (d) 0.025 mol L^{-1} KOCN in DMSO, (e) 0.05 mol L^{-1} NaSCN in DMSO and (f) 0.05 mol L^{-1} KSeCN in DMSO.

what was observed in the 1:2 mole ratio solutions at 2199 cm^{-1} due to a Ni/OCN^- complex species. A peak at 2137 cm^{-1} was also observed which was assigned to the CN stretching frequency of uncomplexed cyanate ion in DMSO.[32]

U.V./Vis data of the Ni(II)/OCN^- model solutions are also summarized in Table II. These indicate in addition to peaks at 276–280 and 412–418 nm, two broad peaks at 602 and 649–656 nm which become more prominent in model solutions with 1:2 mole ratios of Ni(II):OCN^- (and at higher mole ratios in DMSO-based model solutions). These peaks correspond to visible transitions occurring in the complex species formed which are giving rise to the characteristic blue coloration of the solutions. In the 1:1 Ni(II):OCN^- model solutions in DMF or DMSO, the peaks are noticeably weaker or absent which is in agreement with the observed yellow-green or only part blue color of these 1:1 Ni(II):OCN^- solutions.

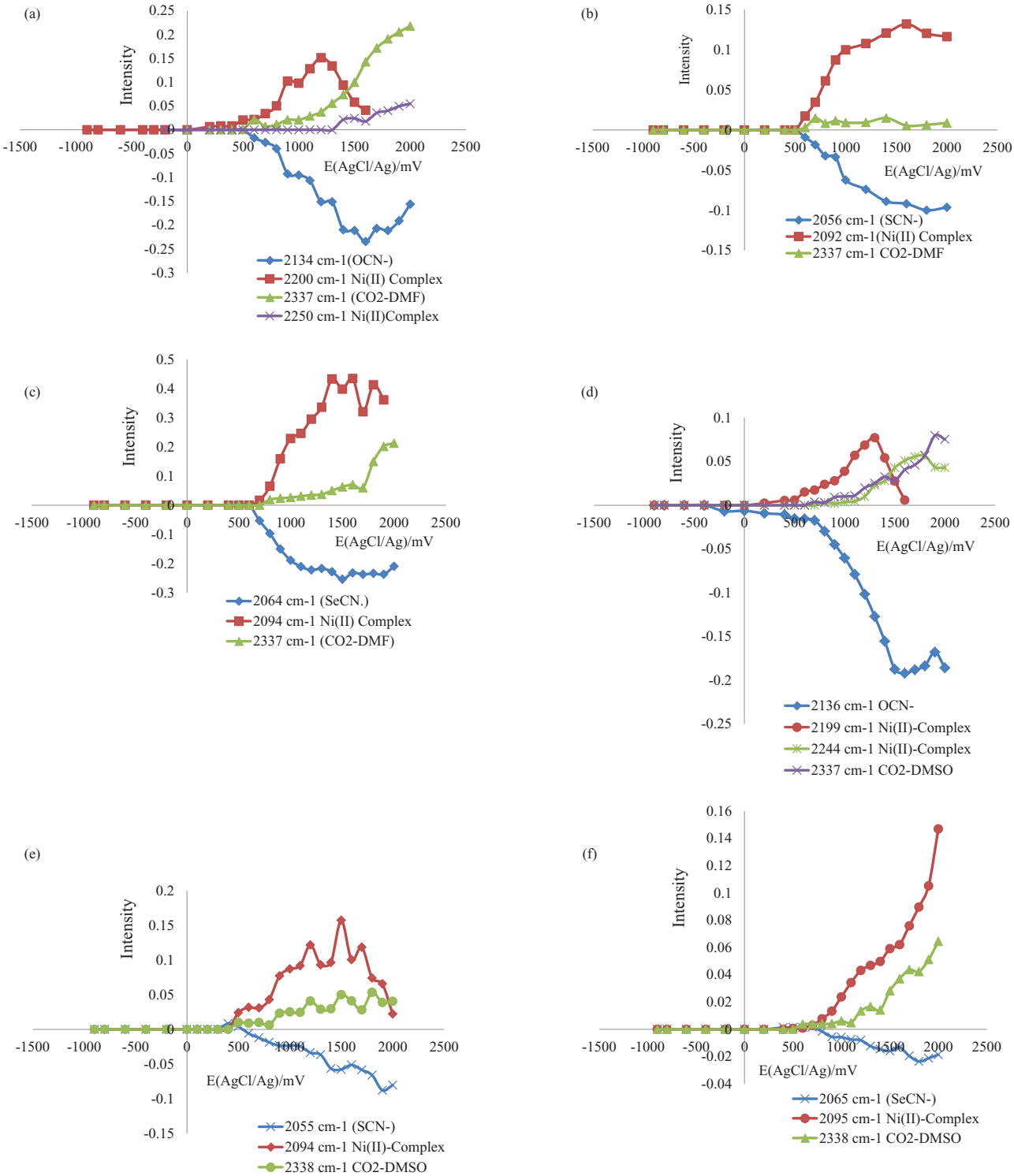

Figure 5. Plots of the intensity changes of the various molecular species generated in the thin layer during electrochemical polarization and observed in the SNIFTIRS spectra as a function of applied potential in the nickel electrode as a function of applied potential in DMF and DMSO solvents containing pseudohalide ions and 0.1 mol L^{-1} TBAP. (a) 0.025 mol L^{-1} KOCN in DMF, (b) 0.05 mol L^{-1} NaSCN in DMF, (c) 0.05 mol L^{-1} KSeCN in DMF, (d) 0.025 mol L^{-1} KOCN in DMSO, (e) 0.05 mol L^{-1} NaSCN in DMSO and (f) 0.05 mol L^{-1} KSeCN in DMSO.

Ni(II)/SCN⁻ and Ni(II)/SeCN⁻ model solutions in DMSO and DMF: FTIR and UV/Vis data.— Model solutions of different Ni(II): SCN^- or $SeCN^-$ mole ratios behaved very similarly to each other in terms of the FTIR and UV/Vis spectra obtained of the solutions and the colors of the solutions obtained. In DMF, two peaks were observed in 1:1 and 1:2 mole ratio Ni(II): SCN^- or $SeCN^-$ solutions, one peak observed at 2094 or 2098 cm^{-1} was due to a Ni/SCN^- or Ni/$SeCN^-$ complex ion species respectively. The other peak observed at 2056 and 2065 cm^{-1} was due to uncomplexed SCN^- and $SeCN^-$ ion respectively in DMF. Peak positions observed by FTIR and UV/Vis were not dependent on the Ni(II):SCN^-/$SeCN^-$ mol ratio in the model solution as in the case of the Ni/OCN^- model solutions. The color of these

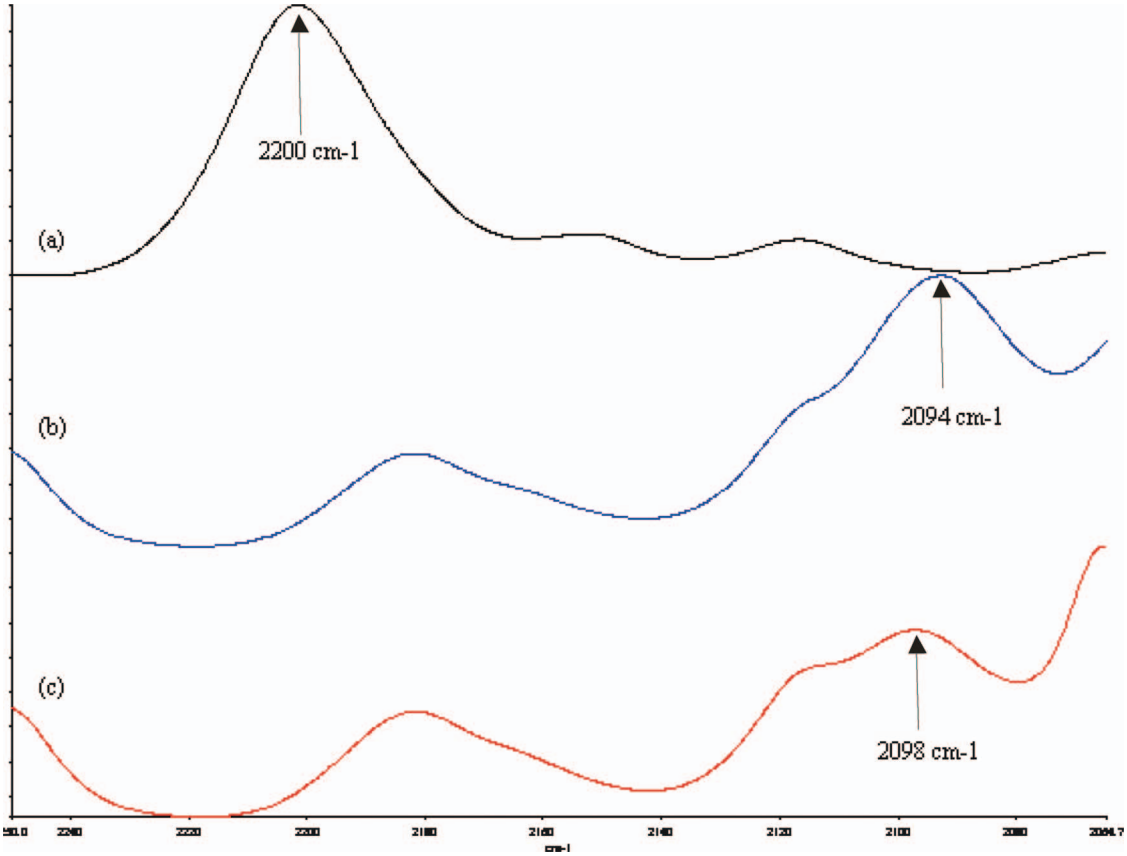

Figure 6. Transmission IR spectra of the various $Ni(NO_3)_2$/pseudohalide salt/ DMF model solutions where $[Ni(NO_3)_2] = 0.025$ mol L^{-1} in each solution. (a) Solution containing a 1:2 $Ni(NO_3)_2$:KOCN mole ratio (blue color), (b) $Ni(NO_3)_2$: NaSCN 1:1 mole ratio solution, (yellow-green color) and (c)) $Ni(NO_3)_2$: KSeCN 1:1 mole ratio (yellow-green color).

solutions were also very similar to each other (i.e. various shades of green to yellow-green) regardless of the Ni(II):SCN^- or $SeCN^-$ mole ratio used in the model solution.

The consistency of colors observed in the model solutions in both solvents of these systems was confirmed by the U.V/Vis data on the systems. In both the Ni(II)/SCN^- and Ni(II)/$SeCN^-$ model solutions regardless of Ni(II):SCN^- or Ni(I):$SeCN^-$ mole ratio, 3 peaks were observed in the ranges 263–297 nm (strong), 401–416 nm (medium) and 677–705 nm (weak).

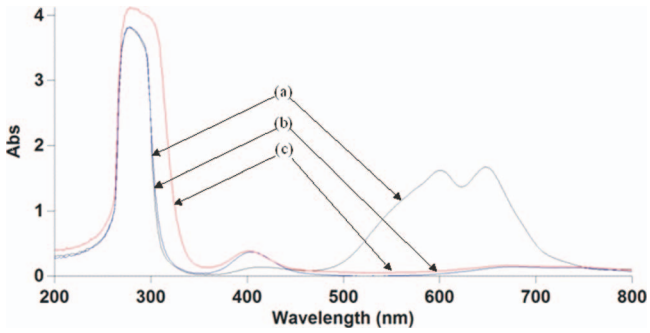

Figure 7. U.V./Vis spectra of the various $Ni(NO_3)_2$/pseudohalide salt/DMF model solutions where $[Ni(NO_3)_2] = 0.025$ mol L^{-1} in each solution. (a) to (c) and arrows provide a guide to the U.V./Vis traces for each system: (a) Solution containing a 1:2 $Ni(NO_3)_2$:KOCN mole ratio (blue color), (b) $Ni(NO_3)_2$: NaSCN 1:1 mole ratio solution, (yellow-green color) and (c)) $Ni(NO_3)_2$: KSeCN 1:1 mole ratio (yellow-green color).

Comparison of the model solution FTIR and UV/Vis data with data from the SNIFTIRS studies of anodic dissolution of Ni in DMSO and DMF solutions containing OCN^-, SCN^- and $SeCN^-$.— Comparison of the vibrational frequencies representing the Ni(II)/pseudohalide complex ion species identified in IR spectra of the model solutions with those obtained from the SNIFTIRS spectra of anodically polarized Ni in these solutions show the species are common to both systems. Additionally, U.V./Vis spectra of the cell solution after the SNIFTIRS experiment showed identical features to those obtained from the model solutions.

FTIR and UV/Vis results alone do not give the exact stoichiometry of the complex ions but provide important clues to be followed up by other techniques. The complex ions in the Ni/SCN^- and Ni/$SeCN^-$ systems were speculated from earlier to be described in terms of a generic, octahedrally coordinated $[Ni(\text{pseudohalide ion})_x(\text{solvent})_{6-x}]^{(2-x)+}$ formula that applies to species formed in both DMF or DMSO. The Ni(II)/cyanate complex ion behaved differently in that it gave a characteristic blue color on formation. Without isolating the complex ions involved as a stable solid and obtaining the crystal structure or else providing more spectroscopic evidence such as an NMR spectrum of the species involved, it is not possible to confirm the stoichiometry. When attempted, it was found impossible to isolate these complex ions from DMSO or DMF and NMR spectra could not be acquired of the complex ions because the Ni^{2+} ion is paramagnetic due to its d^8 electronic configuration thus making it a high spin species with two unpaired electrons.[33] Pilarczyk et al.[25,34] have studied the complexation chemistry of Ni(II) (and other metals) with pseudohalide ions in non-aqueous solvents like DMSO and DMF. They report that the coordination geometry of Ni(II) ions in polar aprotic solvents like DMF is predominantly octahedral and that the pseudohalide ion is N-bonded. Other authors[35] studying addition

of $SeCN^-$ to solutions of Co^{2+} and Ni^{2+} state that Ni^{2+} ion forms a 6-coordinate monoselenocyanato complex $[Ni(DMSO)_5(SeCN)]^+$ with a λ_{max} of 415 nm in agreement with the current study (see Table II).

Ni(II) isocyanato complexes have been found in past studies to behave differently and produce different colored solutions which can be attributed to a difference in coordination geometry. Forster and Goodgame[36,37] isolated crystals of $(Et_4N)_2Ni(NCO)_4$ which were blue in color and exhibited (in nitromethane solutions) intense C≡N IR stretching frequencies of 2208 cm^{-1} in agreement with that observed in the current study. The geometry of the $Ni(NCO)_4^{2-}$ ion in Forster and Goodgame's solutions was reported as tetrahedral based on the infrared spectra. Moreover, Fackler et al.[38] have also stated that DMSO solutions containing $Ni(ClO_4)_2.6H_2O$ and KOCN were intense blue and attributed this to a trisisocyanato Ni(II) or a tetraisocyanato Ni(II) complex. In conclusion it is clear that the Ni(II)/SCN^- and Ni(II)/$SeCN^-$ complex ions generated in solution via anodic dissolution of Ni possess 6-coordinate, possibly octahedral coordination geometry and that IR evidence from model solutions shows that the complexes formed do contain at least one coordinated pseudohalide ligand. Furthermore, Forster and Goodgame[36,37] report that $Ni(NCS)_4^{2-}$ salts are also blue in color hence confirming this ion is not forming in the anodic dissolution experiments in the present study. In contrast, the coordination geometry of the blue Ni(II)/OCN^- complex ions formed via anodic dissolution of Ni in cyanate/DMSO or DMF solutions is demonstrably different. Based on previous data, the stoichiometry of the ion giving rise to the blue color in solutions is most likely to be $Ni(NCO)_4^{2-}$ hence possessing tetrahedral geometry and not octahedral geometry as previously posited for the SCN^- and $SeCN^-$ complex ions. Although this study has presented convincing arguments for elucidating the stoichiometries of the complex ions produced during anodic dissolution, some of the electrode solutions (after conducting SNIFTIRS) and the model solutions in the present study have been subjected to ongoing investigations[27] using alternative in situ techniques such as synchrotron analyzes for providing further insights into the Ni(II)/pseudohalide complex ion stoichiometries and their dynamics.

Conclusions

The study reports the first investigation by SNIFTIRS of the anodic dissolution of nickel electrodes in non-aqueous solutions (DMF or DMSO) of pseudohalide ion-containing electrolytes (i.e. OCN^-, SCN^- and $SeCN^-$) as a function of applied potential. In general, it showed that nickel undergoes irreversible anodic dissolution/corrosion in all systems studied to form complex ion species involving both the respective pseudohalide ion and solvent at relatively high values of the applied potential > +500 mV (AgCl/Ag). In cyanate solutions, nickel dissolves to produce a solution species characterized by an IR peak at 2200 cm^{-1} which has been assigned to a blue-colored Ni(II) cyanate complex which could be $Ni(NCO)_4^{2-}$. In contrast, when the nickel electrode anodically dissolves in thiocyanate-containing or selenocyanate-containing solutions, species giving IR peaks at 2094 cm^{-1} can be assigned to an approximately octahedral Ni(II) thiocyanate/solvent or selenocyanate/solvent complex ion with a suggested formula of $[Ni(NCS)(solvent)_5]^+$ or $[Ni(NCSe)(solvent)_5]^+$ These conclusions were largely supported by model solution IR data and previous literature. Other peaks of interest observed in SNIFTIRS spectra of these systems were those of the free pseudohalide ion which gave negative-going features in spectra at anodic potentials due to its consumption in electrochemical processes. An insoluble nickel-oxide/cyanate film was detected in the Ni/OCN^- systems at highly anodic potentials with contemporaneous detection of solvent-dissolved-CO_2 at 2337–2339 cm^{-1} arising from oxidation of the solvent or pseudohalide ion. CO_2 peaks were also observed in the Ni/SCN^- and Ni/$SeCN^-$ systems but to a lesser extent than in the Ni/OCN^- systems.

Acknowledgments

Emeritus Professor Brian Nicholson and Professor Bill Henderson of the Chemistry Department are warmly acknowledged for advice on the inorganic coordination chemistry of nickel and other transition metal complexes. We are grateful to funding provided (project M-5037) by the New Zealand Synchrotron Group and the Australian Synchrotron in 2012 to carry out in situ work on the electrochemical and model solution systems alluded to in this publication.

References

1. K. Ashley and S. Pons, *Chem. Rev.*, **88**, 673 (1988).
2. K. Ashley, *Talanta*, **38**, 1209 (1991).
3. C. Korzeniewski, in *Handbook of Vibrational Spectroscopy*, J. M. Chalmers and P. R. Griffiths Editors, p. 2700, John Wiley, New York (2002).
4. B. Bozzini, M. Kazemian Abyaneh, B. Busson, G. P. de Gaudenzi, L. Gregoratti, C. Humbert, M. Amati, C. Mele, and A. Tadjeddine, *J. Power Sources*, **231**, 6 (2013).
5. R. M. Souto, F. Ricci, L. Szpyrkowicz, J. L. Rodriguez, and E. Pastor, *J. Phys. Chem. C*, **115**, 3671 (2011).
6. Y.-Y. Yang, J. Ren, H.-X. Zhang, Z.-Y. Zhou, S.-G. Sun, and W.-B. Cai, *Langmuir*, **29**, 1709 (2013).
7. J. M. Smieja, M. D. Sampson, K. A. Grice, E. A. Benson, J. D. Froehlich, and C. P Kubiak, *Inorg. Chem.*, **52**, 2484 (2013).
8. N. Xu, J. Lilly, D. R. Powell, and G. B. Richter-Addo, *Organometallics*, **31**, 827 (2012).
9. C. A. Melendres, G. A. Bowmaker, J. M. Leger, and B. Beden, *J. Electroanal. Chem.*, **449**, 215 (1998).
10. G. A. Bowmaker, J.-M. Leger, A. Le Rille, C. A. Melendres, and A. Tadjeddine, *J. Chem. Soc. Faraday Trans.*, **94**(9), 1309 (1998).
11. K. Brandt, E. Vogler, M. Parthenopoulos, and K. Wandelt, *J. Electroanal. Chem.*, **570**, 47 (2004).
12. M. A. El-Attar, N. Xu, D. Awasabisah, D. R. Powell, and G. B. Richter-Addo, *Polyhedron*, **40**, 105 (2012).
13. M. R. Mucalo and Q. Li, *J. Colloid Interface Sci.*, **269**, 370 (2004).
14. M. R. Mucalo, R. P. Cooney, and G. A. Wright, *J. Chem. Soc. Faraday Trans.*, **86**, 1083 (1990).
15. P. A. Kilmartin and G. A. Wright, *Aust. J. Chem.*, **50**, 321 (1997).
16. M. Bron and R. Holze, *Electrochim. Acta*, **45**, 1121 (1999).
17. M. Bron and R. Holze, *J. Electroanal. Chem.*, **385**, 105 (1995).
18. A. B. Delgado, D. Posadas, and A. J. Arvia, *Electrochim. Acta*, **21**, 385 (1976).
19. F. Bellucci, G. Capobianco, A. Deganello, A. Glisenti, T. Monetta, and G. Moretti, in *Electrochemical Methods in Corrosion Research Vl, Pts 1 and 2*, P. L. Bonora and F. Deflorian Editors, p. 1311, Transtec Publications, Zurich-Uetikon (1998).
20. N. P. Abrashkina, T. R. Agladze, and G. S. Raskin, *Protect. Met.*, **13**, 565 (1977).
21. L. Ercolano, T. Monetta, and F. Bellucci, *Corrosion Sci.*, **35**, 161 (1993).
22. J. Banas, B. Stypula, K. Banas, J. Swiatowska-Mrowiecka, M. Starowicz, and U. Lelek-Borkowska, *J. Solid State Electrochem.*, **13**, 1669 (2009).
23. F. Bellucci, C. A. Farina, and G. Faita, *Electrochim. Acta*, **26**, 731 (1981).
24. K. P. Sarma and R. K. Poddar, *Transit. Met. Chem.*, **9**, 135 (1984).
25. M. Pilarczyk, W. Grzybkowski, and L. Klinszporn, *Bull. Pol. Acad. Sci.-Chem.*, **35**, 559 (1987).
26. P. Krtil, L. Kavan, I. Hoskovcová, and K. Kratochvilová, *Journal of Applied Electrochemistry*, **26**, 523 (1996).
27. L. K. H. K. Alwis, B. Ingham, and M. R. Mucalo, [Unpublished] (2013).
28. R. C. Weast, Ed., *CRC Handbook of Chemistry and Physics*, 65th ed., p. D157, CRC Press, Boca Raton, FL (1984).
29. O. I. Kuntyi, E. V. Okhremchuk, and M. S. Khoma, *Materials Science*, **39**, 885 (2003).
30. B. Mavis and M. Akinc, *Chem Mater.*, **18**, 5317 (2006).
31. P. Krtil, L. Kavan, and P. Novak, *J. Electrochem Soc.*, **140**(2), 3390 (1993).
32. C. L. LeBorgne and M. Chabanel, *J. Molec Liquids*, **73–74**, 171 (1997).
33. F. A. Cotton and G. Wilkinson, *Advanced Inorganic Chemistry: A Comprehensive Text*, pp. 645–787, Wiley, New York (1980).
34. M. Pilarczyk, W. Grzybkowski, and L. Klinszporn, *J. Chem. Soc., Faraday Trans. I*, **85**, 3395 (1989).
35. V. V. Skopenko and I. S. Spivak, *UKR. KHIM. ZH. (Russian Edition)*, **41**, 657 (1975).
36. D. Forster and D. M. L. Goodgame, *Journal of the Chemical Society*, 2790 (1964).
37. D. Forster and D. M. L. Goodgame, *Journal of the Chemical Society*, 262 (1965).
38. J. P. Fackler Jr., G. E. Dolbear, and D. Coucouvanis, *J. Inorg. Nucl. Chem.*, **26**, 2035 (1964).